Available online at www.sciencedirect.com

SciVerse ScienceDirect

Journal of Nutritional Biochemistry 23 (2012) 1230–1237

Journal of Nutritional Biochemistry

The citrus flavonone hesperetin inhibits growth of aromatase-expressing MCF-7 tumor in ovariectomized athymic mice☆

Lan Ye[a], Franky L. Chan[b], Shiuan Chen[c], Lai K. Leung[a,d,*]

[a]Biochemistry Programme, School of Life Sciences, Faculty of Science, the Chinese University of Hong Kong
[b]School of Biomedical Sciences, Faculty of Medicine, the Chinese University of Hong Kong
[c]Division of Immunology, Beckman Research Institute of the City of Hope, Duarte, CA 91010, USA
[d]Food and Nutritional Sciences Programme, School of Life Sciences, Faculty of Science, the Chinese University of Hong Kong

Received 12 January 2011; received in revised form 2 June 2011; accepted 12 July 2011

Abstract

Aromatase is responsible for the rate-determining reaction in estrogen synthesis and is a prime target for treating estrogen-receptor-positive breast cancer. Previous *in vitro* study has demonstrated that apigenin (APG), naringenin (NGN) and hesperetin (HSP) are three of the most potent natural aromatase inhibitors. Because the enzyme inhibition could potentially block breast cancer development, we employed an established postmenopausal breast cancer model to examine the chemopreventive effect of these flavonoids *in vivo*. Athymic mice were ovariectomized and transplanted with aromatase-overexpressing MCF-7 cells. Dietary administration of HSP at 1000 ppm and 5000 ppm significantly deterred the xenograft growth, while a null effect was observed in mice treated with APG or NGN. Further study illustrated that plasma estrogen in HSP-treated mice was reduced. Messenger RNA expression of the estrogen-responsive gene pS2 was also decreased in the tumors of mice treated with 1000 and 5000 ppm HSP. On the other hand, western analysis indicated that cyclin D1, CDK4 and Bcl-x(L) were reduced in the tumors. This study suggested that HSP could be a potential chemopreventive agent against breast carcinogenesis through aromatase inhibition.

Keywords: Hesperetin; Aromatase; Breast cancer cells

1. Introduction

Prolonged exposure to estrogen has been considered a risk factor for breast cancer [1,2]. This causal effect of estrogen exposure was supported in a transgenic model performed recently [3]. Estrogen can be synthesized from cholesterol in several steps involving cytochrome P450 (CYP) 19, and it can be hydroxylated into several metabolites. Among the metabolites, 4-hydroxyestrogen retains the cell proliferative properties of estrogen and can be further metabolized into a carcinogenic moiety as demonstrated in animal models [4–6]. CYP1B1 is responsible for the 4-hydroxylation of estrogen. Therefore, agents that can suppress CYP1B1 and CYP19 may interrupt the natural history of breast cancer development. In spite of its mutagenic potential, estrogen has long been regarded as a cancer promoter. It induces proliferation of breast cancer cells and alters Bcl-2 family protein expression to the favor of antiapoptosis [7].

Estrogen receptor (ER) has been a target for the prevention and treatment of breast cancer. Because of the increased amount of ER found in premalignant and malignant breast tumor, ER is a prognostic parameter of the disease [8]. Although alternate pathways have been suggested, the receptor-mediated nuclear event is still the core of the hormone's physiological action. Therefore, the antiestrogen tamoxifen is usually administered as an adjuvant therapy for receptor-positive breast cancers. Alternatively, CYP19 (aromatase) inhibitors can be administered for purposes of targeting estrogen reduction. One study has found that CYP19 inhibitors can be more effective than tamoxifen in protecting against the development of contralateral breast cancers [9].

CYP19 inhibition is a contemporary treatment for breast cancer. Increased CYP19 expression has been demonstrated in breast cancer tissue, and the estrogen concentration in the tissue is many times higher than the circulation [10]. Santner et al. [11] and Yue et al. [12] have illustrated that locally produced estrogen encourages tumor growth. Lee et al. [13] and Hirose et al. [14] have shown that polymorphisms in the *CYP19* gene are associated with increased risk of breast cancer.

Citrus flavonoids have been shown to be anticancer in cell culture studies [15,16]. Citrus flavonoids and juices also inhibit mammary tumorigenesis induced by 7,12-dimethyl-benz[a]anthracene in female Sprague–Dawley rats [17,18]. Hesperetin (HSP) and naringenin (NGN) are flavonones found abundantly in citrus fruits and have potential anticarcinogenic activity. Hesperetin prevents against 1,2-dimethyl hydrazine-induced colon carcinogenesis in rats [19] and

☆ Conflicts of interest: The authors have no conflicts of interest in this study.

* Corresponding author. Food and Nutritional Sciences Programme, School of Life Sciences, The Chinese University of Hong Kong, Shatin, N.T., Hong Kong. Tel.: +852 26098137; fax: +852 26037732.
E-mail address: laikleung@cuhk.edu.hk (L.K. Leung).

0955-2863/$ - see front matter © 2012 Elsevier Inc. All rights reserved.
doi:10.1016/j.jnutbio.2011.07.003

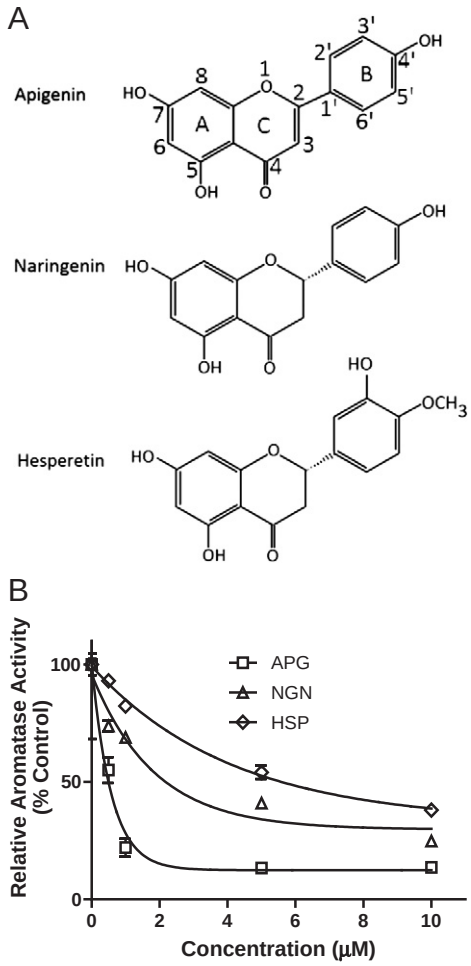

Fig. 1. HSP, NGN and APG Inhibited aromatase activity *in vitro*. MCF-7aro cells were cultured and treated with HSP, NGN or APG for 24 hours before assaying for aromatase activity. Structures of the flavonoids are shown in Fig. 1A. The flavonoids HSP, NGN and APG could inhibit the aromatase with an IC_{50} value of about 5, 2, and 1μM, respectively (Fig.1B). Values are means ± SE, $n = 3$.

inhibited cell proliferation of breast cancer cells through inducing G1 phase arrest [20]. Apigenin (APG) is a flavonoid commonly found in fruit and vegetables, and its anticancer properties have also been documented. It inhibits the growth of breast cancer cells MDA-MB-231 [21] and MDA-MB-453 [22] through caspase-3 activation and apoptosis induction. Chen et al. [23] have also demonstrated its can inhibit MDA-MB-231 xenograft growth *in vivo*.

Hesperetin, NGN and APG are aromatase-inhibiting flavonoids with the highest potency as shown in previous *in vitro* studies [24,25]. However, the *in vivo* effects of these flavonoids have been under scrutiny [26]. Employing a postmenopausal breast cancer model developed by Yue et al. [27], the present study was designed to address the aromatase inhibitory effects of these dietary flavonones *in vivo*.

2. Materials and methods

2.1. Chemicals

Hesperetin, NGN and APG were obtained from Indofine Chemical Co., Inc. (Hillsborough, NJ, USA). Other chemicals, if not stated, were purchased from Sigma Chemicals (St. Louis, MO, USA).

2.2. Cell culture

The breast cancer cell line MCF-7 was purchased from ATCC (Rockville, MD, USA). MCF-7 cells stably transfected with human CYP19 (MCF-7aro) were prepared as previously described [28]. The stably transfected MCF-7 cells were maintained in MEM medium (Invitrogen, Grand Island, NY, USA) supplemented with 10% fetal bovine serum (Invitrogen Life Technology, Rockville, MD, USA) and the selection antibiotic 500 μg/ml G418 (USB, Cleveland, OH, USA). Cells were incubated at 37°C under 5% carbon dioxide atmosphere and routinely subcultured when 80% confluency was reached. Hesperetin was administered in the solvent vehicle dimethyl sulfoxide, and the concentration was limited to 0.1% v/v. Cell density was seeded uniformly at 5×10^2 cells/mm^2 in all experiments.

2.3. Aromatase assays

These assays were performed as previously described [29]. In brief, MCF-7aro cells were seeded and allowed 1 day for attachment. Assays were started by replacing the culture medium with serum-free medium containing [1β-^{3}H(N)]-androst-4-ene-3,17-dione (NET-926; PerkinElmer Life and Analytical Sciences, Boston MA, USA) and HSP. The final concentration of androstenedione was controlled at 25 nM,

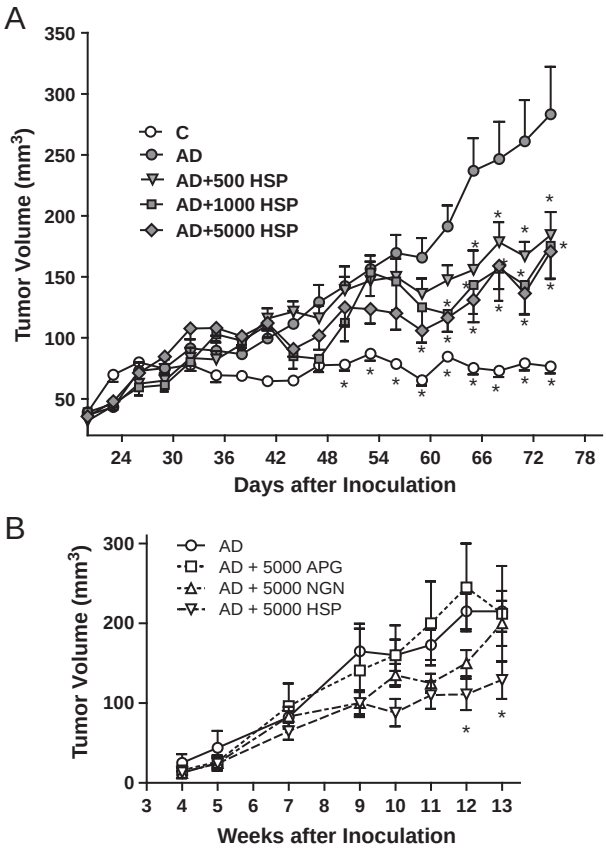

Fig. 2. HSP but not NGN or APG prevented growth of MCF-7aro transplant tumor. Ovariectomized athymic mice were inoculated with MCF-7aro cells and treated with HSP and androstenedione. Volume of the transplant tumor was estimated after inoculation. Tumor sizes in mice receiving HSP are shown in Fig.2A. Groups labeled as C, AD, AD+500, AD+1000, and AD+5000 are mice received solvent vehicle, androstenedione injection, androstenedione injection and dietary HSP at 500 ppm, 1000 ppm, or 5000 pm, respectively. Values are means ± SEM, n=11 to 12. In Fig.2B, groups labeled as AD, AD+5000 NGN, and AD+5000 APG are mice received androstenedione injection, androstenedione injection and 5000 ppm NGN, or 5000 pm APG. Values are means ± SEM, n=4. Means labeled with (*) are significant ($p < 0.05$) lower than that of the group treated solely with androstenedione (AD).

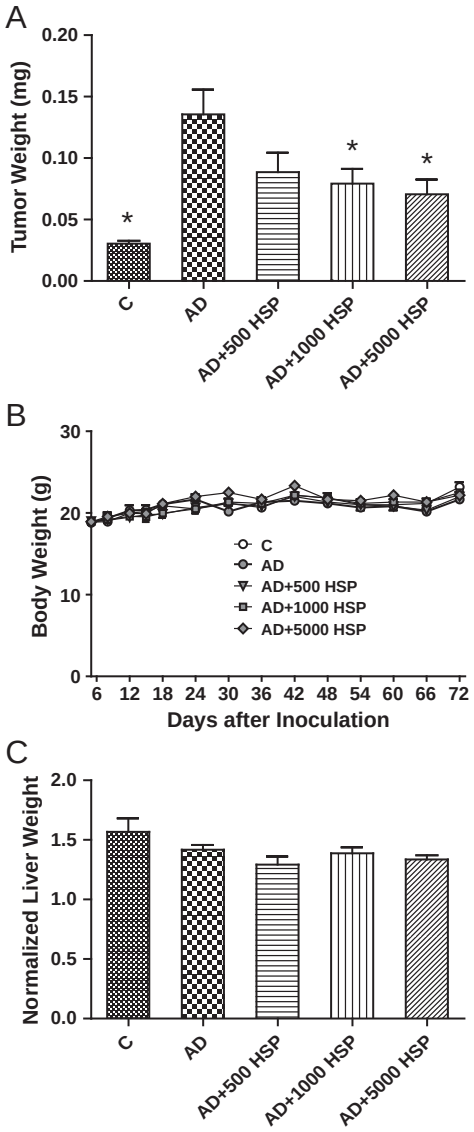

Fig. 3. Tumor, body and liver weight of mice cotreated with androstenedione and HSP. Ovari-ectomized athymic mice were inoculated with MCF-7aro cells and treated with HSP and androstenedione. The tumors were recovered and weighted at the day of sacrifice (Fig. 3A).Their body weight was monitored from the first week after inoculation (Fig. 3B), and liver wet weight was measured at the end of experiment (Fig. 3C). Groups labeled as C, AD, AD+500, AD+1000, and AD+5000 are mice received solvent vehicle, androstenedione injection, androstenedione injection and dietary HSP at 500 ppm, 1000 ppm, or 5000 pm, respectively. Values are means ± SEM.

and the reaction was incubated at 37°C for 1 h. An aliquot of the medium was then mixed with equal volume of chloroform, followed by a 10,000*g* centrifugation at 4°C for 10 min. The aqueous phase was removed into a new tube containing 500 µl of 5% activated charcoal suspension. After 30 min of incubation, an aliquot of the supernatant fraction was taken out for scintillation counting. The protein content of the cells, on the other hand, was determined by using a BCA kit (Sigma Chemicals) after dissolving the cells in 0.5 mol/L NaOH.

2.4. Effect of dietary HSP on MCF-7aro tumor growth in nude mice

2.4.1. Experiment design

This mouse model for postmenopausal breast carcinogenesis was adopted from Yue et al. [27]. Six-week-old female athymic mice were acquired from the Animal Facility of Chinese University of Hong Kong. The mice were ovariectomized and allowed 2 weeks to recover and were fed semipurified and phytoestrogen-free AIN-93G diet. They were randomly assigned into five regimens and transplanted with MCF-7aro cells. Mice were treated with APG, NGN and HSP up to 5000 ppm mixed in diet, and androstenedione (0.1 mg dissolved in 50µl corn oil) was injected subcutaneously every other day throughout the experiment. Control mice received corn oil injection only. Before transplantation, MCF-7aro cells were maintained in culture incubator as described above. The cells were trypsinized and suspended in matrigel matrix (BD Biosciences, San Jose, CA, USA) (10 mg/ml). A total of 0.1 ml of cells (3×10^7 cells/ml) was injected into the two flanks of the animal. The body weight, tumor size and food intake

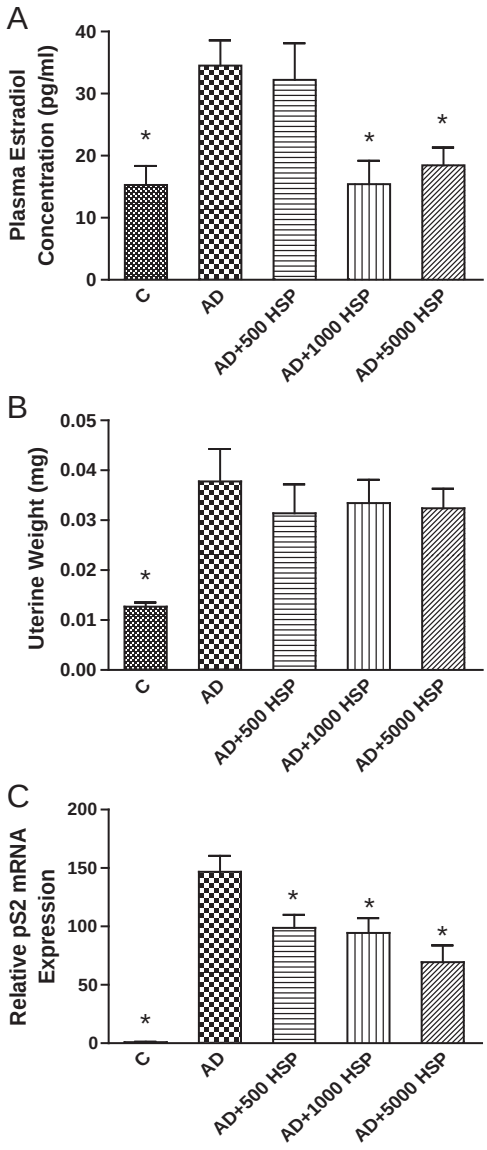

Fig. 4. Serum estradiol concentration, uterine weight, and the estrogen-responsive pS2 mRNA expression in the MCF-7aro xenografts. Blood was drawn from the animals at sacrifice, and estradiol concentration was quantified by ELISA (Fig. 4A). Two estrogen-sensitive tissues were dissected and assayed. Uteri of the experimental animals were weighed at sacrifice (Fig. 4B), and pS2 mRNA expression was quantified in the recovered tumors (Fig. 4C). Groups labeled as C, AD, AD+500, AD+1000, and AD+5000 are mice received solvent vehicle, androstenedione injection, androstenedione injection and dietary HSP at 500 ppm, 1000 ppm, or 5000 pm, respectively. Values are means ± SEM, $n=6$. Means labeled with (*) are significantly different from androstenedione-treated group (AD).

were monitored weekly throughout the study. Tumor volume was measured by an electronic caliper and estimated according to the following formula: $\pi/(6\times\text{length}\times\text{width}\times\text{height})$, where length, width and height were the three orthogonal diameters of the tumors. At the end of the study, the mice were sacrificed by cervical dislocation. Livers and uteri were weighed. Tumors and serum were collected and stored at −80°C until assayed. The procedure was approved by the Animal Experimentation Ethics Committee, Chinese University of Hong Kong.

2.5. Serum estradiol (E2) determination

Serum E2 concentration was measured using E2 enzyme-linked immunosorbent assay (ELISA) kit (Cayman Chemical Company, Ann Arbor, MI, USA). The samples were added into a 96-well plate coated with antibody raised against E2. After incubation and development at room temperature, the absorbance at 410 nm was quantitated using a microplate reader (FluroStar; BMG Labtechnologies GmBH, Offenburg, Germany). The amount of E2 could be read against a standard curve constructed with the E2 standard provided in the kit.

2.6. Measurement of gene expression by quantitative real-time polymerase chain reaction (PCR) assay

Frozen tumors were pulverized in a Dounce homogenizer. Liquid nitrogen was constantly added to keep the tissue in the frozen state throughout the homogenization. Total RNA was extracted from the sample using TRIzol reagent (Invitrogen, Carlsbad, CA, USA). First DNA strand was synthesized from 3 μg of total RNA with oligo dT primers and Moloney murine leukemia virus RT (M-MLV RT; USB Corp., Cleveland, OH, USA). Target fragments were quantified by real-time PCR, and a DNA Engine Opticon2 (MJ Research, Watertown, MA, USA) was employed for this assay. Taqman-VIC MGB probes and primers (Assay-on-Demand) and real-time PCR Taqman Universal PCR Master Mix were all obtained from Applied Biosystems (Foster City, CA, USA). Signals obtained for GAPDH were used as a reference housekeeping gene to normalize the amount of total RNA amplified in each reaction. Relative gene expression data were analyzed using the $2^{-\Delta\Delta CT}$ method [30].

2.7. Western blotting

The pulverized samples were sonicated in lysis buffer [phosphate-buffered saline, 1% NP40, 0.5% sodium deoxycholate, 0.1% sodium dodecyl sulfate (SDS), 40 mg/L phenylmethylsulfonyl fluoride, 0.5 mg/L aprotinin, 0.5 mg/L leupeptin, 1.1 mmol/L EDTA and 0.7 mg/L pepstatin] with a cell disruptor (Branson Ultrasonics Corp., Danbury, CT, USA) on ice for 30 s. Thirty micrograms of homogenized protein was separated on 10% SDS–polyacrylamide gel electrophoresis and transferred onto an Immobilon PVDF membrane (Millipore, Bedford, MA, USA). Anti-CYP19 (Abcam plc, Cambridge, UK), anti-Bcl-xL, anti-Bax, anti-Bak, anti-P21, anti-P57^{kip2}, anti-cyclin A, anti-cyclin D, anti-cyclin E (Santa Cruz Biotechnology, Santa Cruz, CA, USA), anti-actin primary (Sigma Chem) and secondary antibodies conjugated with horseradish peroxidase (Santa Cruz Biotechnology) were used for protein detection. An ECL Detection Kit (Amersham, Arlington Heights, IL, USA) provided the chemiluminescence substrate for horseradish peroxidase, and the targeted protein was visualized by autoradiography. The software ImageJ 1.37v (National Institutes of Health, USA) was employed for optical density measurement.

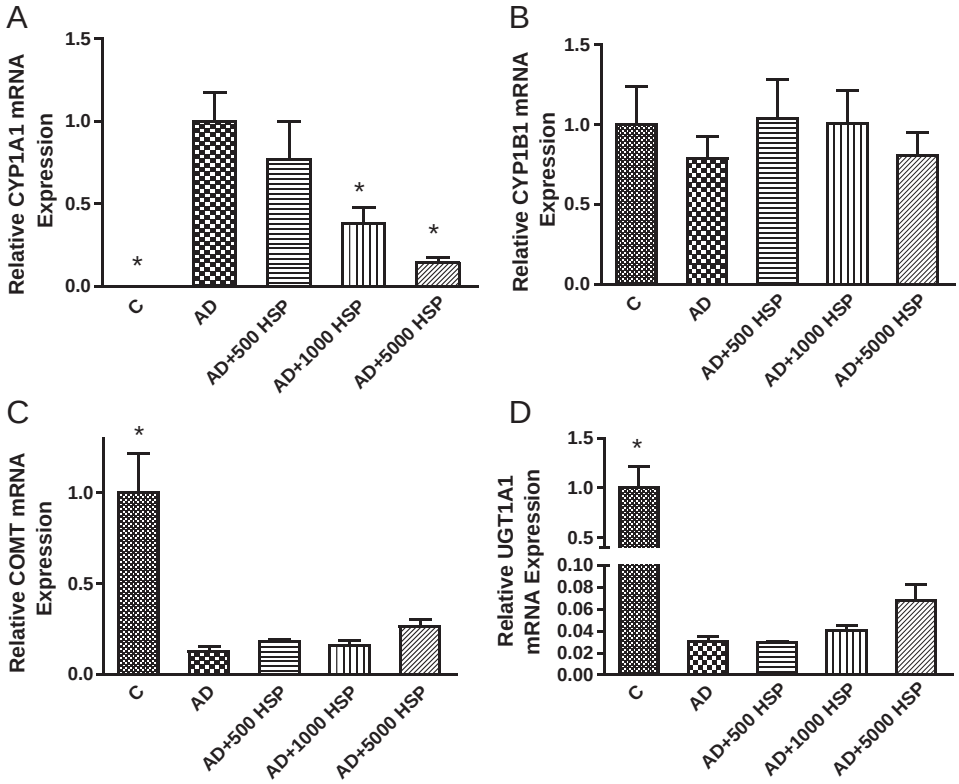

Fig. 5. Messenger RNA levels of estrogen metabolism-related genes in MCF-7aro tumors. Total mRNA was extracted from tumors and messenger RNA expression of estrogen metabolism related genes was quantified by real-time PCR. Groups labeled as C, AD, AD+500, AD+1000, and AD+5000 are mice received solvent vehicle, androstenedione injection, androstenedione injection and dietary HSP at 500 ppm, 1000 ppm, or 5000 pm, respectively. Values are means ± SEM, n=5 to 6 Means labeled with (*) are significantly different from AD.

2.8. Statistical analysis

For the *in vitro* studies, the data were analyzed by the software package Prizm5 (GraphPad Software, Inc., San Diego, CA, USA). One-way analysis of variance (ANOVA) with Dunnett's post hoc test was used for multigroup comparisons. For the tumor volume growth data, two-way ANOVA was employed for analysis.

3. Results

3.1. Enzyme inhibition assay

The chemical structures of HSP, NGN and APG highly resemble each other (Fig. 1A). Hesperetin, NGN and APG inhibited aromatase activity with IC_{50} value of about 5, 2 and 1 μM, respectively (Fig. 1B). Apigenin appeared to be the most potent among the three tested flavonoids.

3.2. Effect of dietary HSP on xenograft growth in ovariectomized mice

An accelerated growth of MCF-7aro tumor was demonstrated in mice treated with androstenedione injection (AD) as compared with the control (C) group. Significant ($P<.05$) deviation in tumor size between these two groups was observed starting from day 50 until sacrifice. Starting from days 65, 62, and 59 after implantation, the respective tumor volumes in mice fed with 500, 1000 and 5000 ppm HSP were significantly ($P<.05$) smaller than those in AD mice (Fig. 2A). Subsequently, APG and NGN were also examined using the same

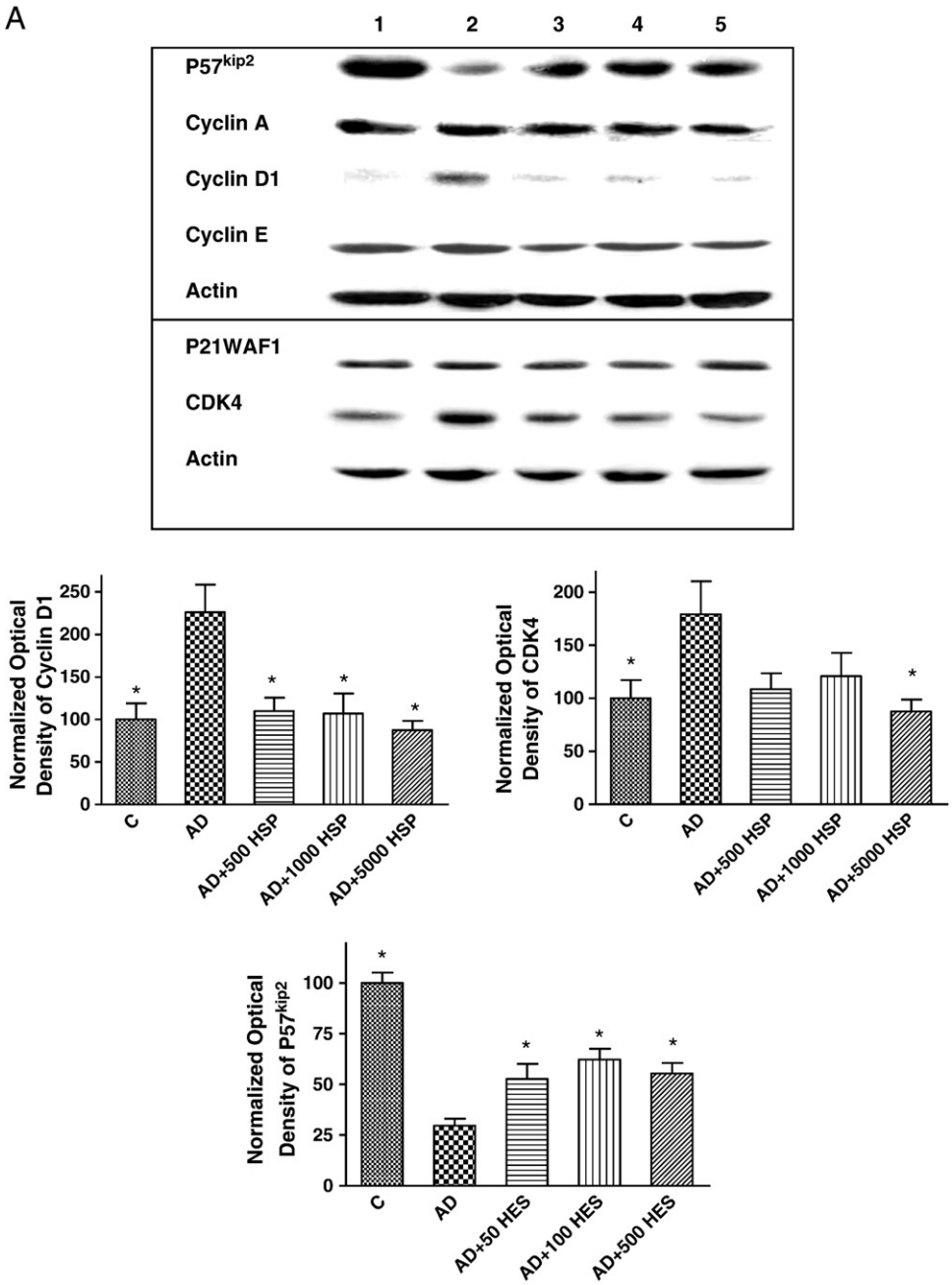

Fig. 6. Immunoblot of apoptosis and cell cycle-regulated genes in tumors. Expressions of cell cycle - (Fig. 6A) and apoptosis (Fig. 6B) - regulated proteins were determined by western blot analysis. The corresponding optical density readings are shown below the image. The image is a representation of 3 to 4 independent experiments with similar results. Means labeled with (*) are significantly different from AD.

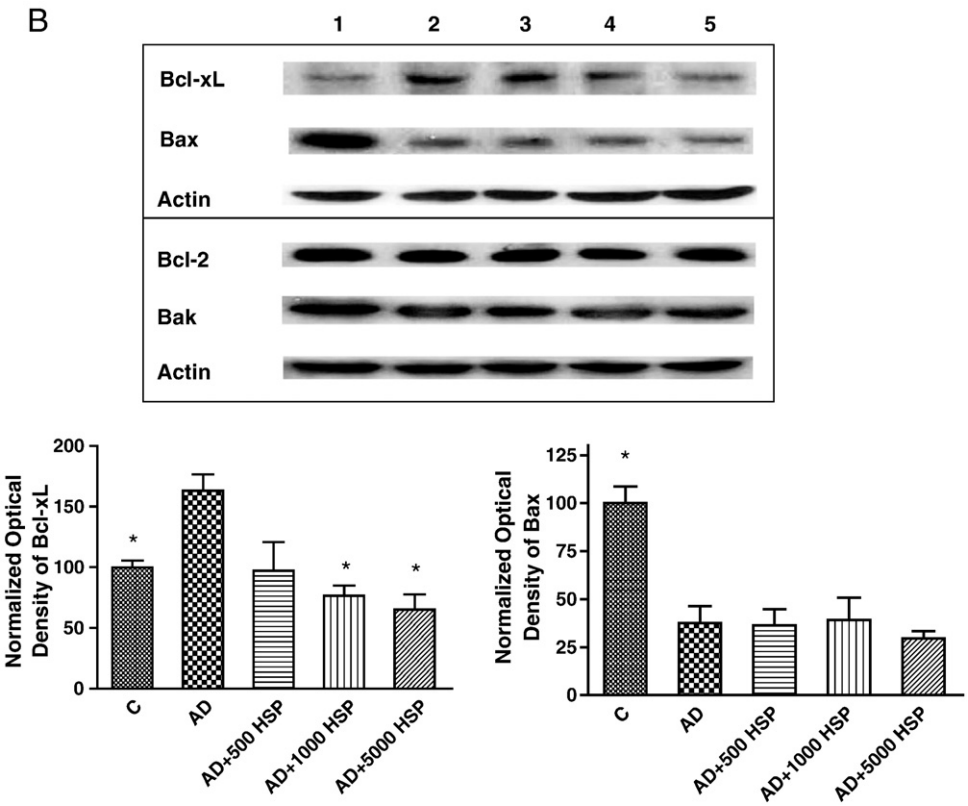

Fig. 6 (*continued*).

model. However, dietary administration of 5000 ppm APG or NGN failed to deter the xenograft growth (Fig. 2B). This experiment demonstrated that the flavonoids' actions *in vivo* were different from those *in vitro*. Feed intake was comparable among the treatment groups (data not shown). The injection of androstenedione and diet treatment appeared to be within the tolerable limit.

3.3. Murine body weight, and liver and tumor wet weights in HSP treatment group

Similar to the estimated tumor volume result, the tumor weight from mice treated with 1000 and 5000 ppm was lighter ($P<.05$) than that from AD mice (Fig. 3A).

No significant differences in mice body weight (Fig. 3B) or liver wet weight (Fig. 3C) were observed among the five groups. These measurements in mice under APG and NGN treatments were not different from those in the AD control group (data not shown).

3.4. Plasma estrogen levels, uterine weight and estrogen-responsive gene expression in tumors of HSP-treated mice

3.4.1. Plasma E2

Increased E2 concentration in serum was seen in AD mice as compared with controls, and the concentration was suppressed by the coadministration of 1000 or 5000 ppm HSP in diet (Fig. 4A). The increased serum E2 could be synthesized from androstenedione in the tumor or the mouse tissues.

3.4.2. pS2 messenger RNA (mRNA) expression in tumor

pS2 expression was increased by 140-fold in AD mice when compared to C mice (Fig. 4B). Dietary HSP treatment significantly ($P<.05$) inhibited pS2 expression induced by the exogenous androstenedione.

3.4.3. Uterine wet weight

The uterine wet weight of AD mice was threefold heavier than that of C mice. Dietary HSP treatment (500, 1000 and 5000 ppm) did not significantly change the uterine wet weight (Fig. 4C). This result suggested that HSP may have uterotrophic action, i.e., the chemical interacted directly with uterine ER to prevent the uterine shrinkage.

3.5. Estrogen metabolism-related gene expression in tumors

Since the metabolism of E2 might also alter the amount in serum, RNA expressions for genes that were crucial to such metabolism were evaluated in the recovered tumors. CYP1A1 expression was significantly induced by androstenedione administration, and cotreatment with HSP repressed the increase (Fig. 5A). No change was observed in CYP1B1 (Fig. 5B) expression, whereas COMT (Fig. 5C) and UGT1A1 (Fig. 5D) expressions were drastically reduced by androstenedione treatment. Hesperetin coadministration did not revert any of these expressions.

3.6. Apoptosis and cell-cycle-regulated proteins

3.6.1. Cell cycle proteins

Cyclin D1 and CDK4 expressed in tumors of AD group were higher than those in the C group, and the induced protein expressions were mostly suppressed by 5000 ppm HSP treatment as shown in Fig. 6A. On the other hand, $P57^{kip2}$ in tumor was reduced by androstenedione treatment, and HSP cotreatment reverted some of the hormonal effect. We observed no statistical differences in the optical density

data of cyclin A, cyclin E and $P21^{WAF1}$ protein expression among the five groups (not shown).

3.6.2. Apoptotic proteins

Western analysis indicated that androstenedione administration induced Bcl-xL expression (Fig. 6B); 1000-ppm and 5000-ppm HSP treatment counteracted the induction. The proapoptotic protein Bax was reduced by androstenedione treatment, and HSP cotreatment had no effect on the expression (Fig. 6B). No changes were observed for Bcl-2 and Bak protein expression (Fig. 6B).

4. Discussion

In the present study, we utilized an ovariectomized nude mouse model to evaluate the effect of dietary HSP, APG and NGN on breast carcinogenesis. Unlike their *in vitro* results, only HSP retained the inhibitory effect *in vivo*. The observation that NGN and APG failed to show their aromatase inhibition *in vivo* was consistent with that from a previous report [26].

In the *in vitro* results of the present study, the aromatase-inhibitory potencies of the three tested flavonoids were slightly different. The C2 position of NGN is an *sp3* instead of *sp2* hybridization structure as seen in APG. This sole structural difference between these two flavonoids might account for the reduced potency in NGN. Hesperetin, on the other hand, has two structural differences when compared to NGN. Hesperetin has a 3′-OH group and a methoxyl group instead of hydroxyl group at the 4′ position, and HSP was a less potent aromatase inhibitor than NGN in the present study. However, the 4′ methoxyl group was not likely to be a contributing factor. An analogous structure disparity at the 4′ position is seen in biochanin A and genistein, and our lab has previously shown that biochanin A has a greater aromatase inhibitory activity than genistein [31].

As illustrated before [32], growth of MCF-7aro xenograft in this model was stimulated by estrogen synthesized locally similar to most postmenopausal breast cancers. Dietary HSP counteracted the synthesis of estrogen and suppressed the xenograft growth. An increase in circulating E2 level was observed in androstenedione-induced mice, and HSP cotreatment reduced the hormone concentration. The expression of estrogen-sensitive gene pS2 in the tumors fully complied with the serum hormone concentration. However, the uterine wet weight appeared to be consistent with the serum E2 concentration in AD mice only. In spite of reduction in serum E2, the induced uterine weight was not reduced in HSP cotreatment groups. This can be explained by the differential responsiveness of the tissues toward estrogen and HSP. The weak estrogenic property of HSP was also demonstrated (data not shown). Alternatively, the estrogen concentration at the site of synthesis, i.e., the xenograft, should be higher than that in the circulation. The concentration differences in the tumors from HSP-treated mice were adequate to induce changes in pS2 expression.

COMT and UGT1A1 facilitate the elimination of estrogen. Suppression on COMT and UGT1A1 expression might partially contribute to the increase of estrogen concentration and stimulate tumor growth in groups treated with androstenedione. Walle and Walle [33] have reported that flavonoids such as chrysin, acacetin, APG, luteolin and diosmetin are inducers of UGT1A1. However, HSP did not suppress the expression of UGT in the current study.

Previous study has demonstrated that HSP is an inhibitor of CYP1A1 [34]. This enzyme hydroxylates estrogen and facilitates its subsequent elimination. In the present study, HSP treatment suppressed rather than increased CYP1A1 expression. This result does not support the notion that HSP reduced the circulating estrogen through deactivation or elimination.

Hesperetin has been shown to be able to induce G1 phase arrest in MCF-7 cells [20]. Cyclin D1 is an important regulatory protein involved in the G1 phase of cell cycle, and its expression is always increased in many cancers [35]. Estrogen has been reported to induce breast cancer cell proliferation via stimulating G(1)/S transition through increased expression of cyclin D1 and CDKs [36]. The expression pattern of these cell cycle proteins resulting from estrogen administration was observed in AD mice. In addition, the CDK inhibitory protein $P57^{Kip2}$ was down-regulated. The cotreatment of HSP could reverse the expression of these genes.

Estrogen may also alter Bcl-2 family gene expression in favor of cell survival [7,37]. Two estrogen responsive elements have been located and demonstrated to be functional in the promoter of Bcl-2 [38]. Bak and Bcl-x are also down-regulated in estrogen-treated MCF-7 cells [7]. Nevertheless, Bcl-xL was the only Bcl-2 family protein altered in the xenograft. Differences in the growth conditions could lead to the variation in expressions.

Many phytochemicals have been identified to be aromatase inhibitors, such as biochanin A [31], isoliquiritigenin [39], butein [40], resveratrol [41], mushroom extract [29], etc. Most of these compounds have not been tested in animal model except isoliquiritigenin and mushroom extract. Hesperetin is abundant in citrus fruits and common for human consumption. It has the advantage over the other compounds in the ease of isolation and safeness for consumption.

The bioavailability of HSP in the present study was not known. Because of the differences in time and amount of feed consumption, the plasma level of HSP would vary over a large range in the 24-h span. A pharmacokinetic study of hesperidin, the glycoside of HSP, has been carried out in a rodent model [42]. Hesperidin is absorbed in the form of HSP, and the majority would be conjugated to glucuronide in plasma. The peak of plasma concentration of all HSP metabolites is ~0.8 μM at 4 h after oral dosing with 100 mg hesperidin/kg. Another study has shown that the aglycone HSP represents around 4% of total HSP metabolites in rodent plasma, and the others are HSP-7-*O*-glucuronide (55%), HSP sulphate (2%), homoeriodictyol (3%) and homoeriodictyol glucuronides (36%) [43]. By extrapolating all these information, the highest possible plasma concentration of unconjugated HSP in the 1000- and 5000-ppm HSP groups should be around 0.2 and 1 μM, respectively, in the current study. Yet, it is not known whether other metabolites of HSP could inhibit aromatase.

In conclusion, our results demonstrated that dietary treatments of HSP inhibited aromatase enzyme activity and suppressed proliferation of MCF-7aro cells *in vivo*. It prevented the xenograft growth by down-regulating the expression of cyclin D1, CDK4 and Bcl-xL and up-regulating $p57^{Kip2}$ expression. Many of these genes were estrogen responsive. Since this model has been developed for studying breast carcinogenesis in postmenopausal women, HSP could be a potential chemopreventive agent against such disease.

References

[1] Colditz GA. Hormones and breast cancer: evidence and implications for consideration of risks and benefits of hormone replacement therapy. J Womens Health 1999;8:347–57.
[2] Key T, Appleby P, Barnes I, Reeves G. Endogenous sex hormones and breast cancer in postmenopausal women: reanalysis of nine prospective studies. J Natl Cancer Inst 2002;94:606–16.
[3] Yoshidome K, Shibata MA, Couldrey C, Korach KS, Green JE. Estrogen promotes mammary tumor development in C3(1)/SV40 large T-antigen transgenic mice: paradoxical loss of estrogen receptoralpha expression during tumor progression. Cancer Res 2000;60:6901–10.
[4] Liehr JG, Fang WF, Sirbasku DA, Ari-Ulubelen A. Carcinogenicity of catechol estrogens in Syrian hamsters. J Steroid Biochem 1986;24:353–6.
[5] Li JJ, Li SA. Estrogen carcinogenesis in Syrian hamster tissues: role of metabolism. Fed Proc 1987;46:1858–63.

[6] Zhu BT, Conney AH. Functional role of estrogen metabolism in target cells: review and perspectives. Carcinogenesis 1998;19:1–27.
[7] Leung LK, Wang TT. Paradoxical regulation of Bcl-2 family proteins by 17beta-oestradiol in human breast cancer cells MCF-7. Br J Cancer 1999;81:387–92.
[8] Sommer S, Fuqua SA. Estrogen receptor and breast cancer. Semin Cancer Biol 2001;11:339–52.
[9] Kudachadkar R, O'Regan RM. Aromatase inhibitors as adjuvant therapy for postmenopausal patients with early stage breast cancer. CA Cancer J Clin 2005;55: 145–63.
[10] Miller WR, Dixon JM. Local endocrine effects of aromatase inhibitors within the breast. J Steroid Biochem Mol Biol 2001;79:93–102.
[11] Santner SJ, Chen S, Zhou D, Korsunsky Z, Martel J, Santen RJ. Effect of androstenedione on growth of untransfected and aromatase-transfected MCF-7 cells in culture. J Steroid Biochem Mol Biol 1993;44:611–6.
[12] Yue W, Santner SJ, Masamura S, Wang JP, Demers LM, Hamilton C, et al. Determinants of tissue estradiol levels and biologic responsiveness in breast tumors. Breast Cancer Res Treat 1998;49(Suppl 1):S1–7 discussion S33–7.
[13] Lee KM, Abel J, Ko Y, Harth V, Park WY, Seo JS, et al. Genetic polymorphisms of cytochrome P450 19 and 1B1, alcohol use, and breast cancer risk in Korean women. Br J Cancer 2003;88:675–8.
[14] Hirose K, Matsuo K, Toyama T, Iwata H, Hamajima N, Tajima K. The CYP19 gene codon 39 Trp/Arg polymorphism increases breast cancer risk in subsets of premenopausal Japanese. Cancer Epidemiol Biomarkers Prev 2004;13:1407–11.
[15] Benavente-Garcia O, Castillo J, Alcaraz M, Vicente V, Del Rio JA, Ortuno A. Beneficial action of citrus flavonoids on multiple cancer-related biological pathways. Curr Cancer Drug Targets 2007;7:795–809.
[16] Manthey JA, Guthrie N. Antiproliferative activities of citrus flavonoids against six human cancer cell lines. J Agric Food Chem 2002;50:5837–43.
[17] So FV, Guthrie N, Chambers AF, Moussa M, Carroll KK. Inhibition of human breast cancer cell proliferation and delay of mammary tumorigenesis by flavonoids and citrus juices. Nutr Cancer 1996;26:167–81.
[18] Guthrie N, Carroll KK. Inhibition of mammary cancer by citrus flavonoids. Adv Exp Med Biol 1998;439:227–36.
[19] Aranganathan S, Panneer Selvam J, Nalini N. Hesperetin exerts dose dependent chemopreventive effect against 1,2-dimethyl hydrazine induced rat colon carcinogenesis. Invest New Drugs 2008.
[20] Choi EJ. Hesperetin induced G1-phase cell cycle arrest in human breast cancer MCF-7 cells: involvement of CDK4 and p21. Nutr Cancer 2007;59:115–9.
[21] Mak P, Leung YK, Tang WY, Harwood C, Ho SM. Apigenin suppresses cancer cell growth through ERbeta. Neoplasia 2006;8:896–904.
[22] Choi EJ, Kim GH. Apigenin induces apoptosis through a mitochondria/caspase-pathway in human breast cancer MDA-MB-453 cells. J Clin Biochem Nutr 2009;44:260–5.
[23] Chen D, Landis-Piwowar KR, Chen MS, Dou QP. Inhibition of proteasome activity by the dietary flavonoid apigenin is associated with growth inhibition in cultured breast cancer cells and xenografts. Breast Cancer Res 2007;9:R80.
[24] Jeong HJ, Shin YG, Kim IH, Pezzuto JM. Inhibition of aromatase activity by flavonoids. Arch Pharm Res 1999;22:309–12.
[25] van Meeuwen JA, Nijmeijer S, Mutarapat T, Ruchirawat S, de Jong PC, Piersma AH, et al. Aromatase inhibition by synthetic lactones and flavonoids in human placental microsomes and breast fibroblasts — a comparative study. Toxicol Appl Pharmacol 2008;228:269–76.
[26] Saarinen N, Joshi SC, Ahotupa M, Li X, Ammala J, Makela S, et al. No evidence for the in vivo activity of aromatase-inhibiting flavonoids. J Steroid Biochem Mol Biol 2001;78:231–9.
[27] Yue W, Zhou D, Chen S, Brodie A. A new nude mouse model for postmenopausal breast cancer using MCF-7 cells transfected with the human aromatase gene. Cancer Res 1994;54:5092–5.
[28] Zhou DJ, Pompon D, Chen SA. Stable expression of human aromatase complementary DNA in mammalian cells: a useful system for aromatase inhibitor screening. Cancer Res 1990;50:6949–54.
[29] Grube BJ, Eng ET, Kao YC, Kwon A, Chen S. White button mushroom phytochemicals inhibit aromatase activity and breast cancer cell proliferation. J Nutr 2001;131:3288–93.
[30] Livak KJ, Schmittgen TD. Analysis of relative gene expression data using real-time quantitative PCR and the 2(−Delta Delta C(T)) method. Methods 2001;25: 402–8.
[31] Wang Y, Man Gho W, Chan FL, Chen S, Leung LK. The red clover (*Trifolium pratense*) isoflavone biochanin A inhibits aromatase activity and expression. Br J Nutr 2008;99:303–10.
[32] Yue W, Brodie A. MCF-7 human breast carcinomas in nude mice as a model for evaluating aromatase inhibitors. J Steroid Biochem Mol Biol 1993;44:671–3.
[33] Walle UK, Walle T. Induction of human UDP-glucuronosyltransferase UGT1A1 by flavonoids-structural requirements. Drug Metab Dispos 2002;30:564–9.
[34] Doostdar H, Burke MD, Mayer RT. Bioflavonoids: selective substrates and inhibitors for cytochrome P450 CYP1A and CYP1B1. Toxicology 2000;144: 31–8.
[35] Hiyama H, Iavarone A, LaBaer J, Reeves SA. Regulated ectopic expression of cyclin D1 induces transcriptional activation of the cdk inhibitor p21 gene without altering cell cycle progression. Oncogene 1997;14:2533–42.
[36] Foster JS, Henley DC, Bukovsky A, Seth P, Wimalasena J. Multifaceted regulation of cell cycle progression by estrogen: regulation of Cdk inhibitors and Cdc25A independent of cyclin D1-Cdk4 function. Mol Cell Biol 2001;21:794–810.
[37] Lee Y, Renaud RA, Friedrich TC, Gorski J. Estrogen causes cell death of estrogen receptor stably transfected cells via apoptosis. J Steroid Biochem Mol Biol 1998;67:327–32.
[38] Perillo B, Sasso A, Abbondanza C, Palumbo G. 17beta-Estradiol inhibits apoptosis in MCF-7 cells, inducing bcl-2 expression via two estrogen-responsive elements present in the coding sequence. Mol Cell Biol 2000;20:2890–901.
[39] Ye L, Gho WM, Chan FL, Chen S, Leung LK. Dietary administration of the licorice flavonoid isoliquiritigenin deters the growth of MCF-7 cells overexpressing aromatase. Int J Cancer 2009;124:1028–36.
[40] Wang Y, Chan FL, Chen S, Leung LK. The plant polyphenol butein inhibits testosterone-induced proliferation in breast cancer cells expressing aromatase. Life Sci 2005;77:39–51.
[41] Wang Y, Lee KW, Chan FL, Chen S, Leung LK. The red wine polyphenol resveratrol displays bilevel inhibition on aromatase in breast cancer cells. Toxicol Sci 2006;92:71–7.
[42] Matsumoto H, Ikoma Y, Sugiura M, Yano M, Hasegawa Y. Identification and quantification of the conjugated metabolites derived from orally administered hesperidin in rat plasma. J Agric Food Chem 2004;52:6653–9.
[43] Habauzit V, Nielsen IL, Gil-Izquierdo A, Trzeciakiewicz A, Morand C, Chee W, et al. Increased bioavailability of hesperetin-7-glucoside compared with hesperidin results in more efficient prevention of bone loss in adult ovariectomised rats. Br J Nutr 2009;102:976–84.